



Electron Probe Microanalysis: A Review of the Past, Present, and Future

Romano Rinaldi,^{1,*} and Xavier Llovet²

¹*ex Dipartimento di Scienze della Terra (now Physics and Geology), Università di Perugia, 06123 Perugia, Italy*

²*Scientific and Technological Centers (CCiTUB), Universitat de Barcelona, Lluís Solé Sabarís 1-3, 08028 Barcelona, Spain*

Abstract: The 50th anniversary of the application of electron probe microanalysis (EPMA) to the Earth Sciences provides an opportunity for an assessment of the state-of-the-art of the technique. Stemming from the introduction of the first automated instruments, the latest developments of EPMA and some typical applications are reviewed with an eye to the future. The most noticeable recent technical achievements such as the field-emission electron gun, the latest generation of energy and wavelength dispersive spectrometers, and the development of analytical methods based on new sets of first principle data obtained by the use of sophisticated computer codes, allow for the extension of the method to the analysis of trace elements, ultra-light elements (down to Li), small particles, and thin films, with a high degree of accuracy and precision and within a considerably reduced volume of interaction. A number of working examples and a thorough list of references provide the reader with a working knowledge of the capabilities and limitations of EPMA today.

Key words: electron probe microanalysis, X-ray spectrometry, latest developments, capabilities and limitations, future developments

A BRIEF HISTORY FROM A PERSONAL PERSPECTIVE

The Early Days

In 2001, on the 50th anniversary of electron probe microanalysis (EPMA), Peter Duncumb published in this Journal a fascinating account of the early days dealing with the first 10 years of the technique when “there were still fewer than 20 instruments in existence or under construction around the world” (Duncumb, 2001). His account narrated the design requirements that inspired the various first-generation instruments and showed how the later commercialization had to converge over a few variants to reconcile the many conflicting requirements.

Fourteen years after Duncumb’s paper, we can consider this year the 50th anniversary of electron microprobe applications in the Earth Sciences and in particular its widespread use in determinative mineralogy. The main manufactures of dedicated EPMA instruments are now only two, but the practice of EPMA has expanded to all electron beam instruments, mostly thanks to the development of energy dispersive spectrometry (EDS), microelectronics, and computer capabilities.

In the Fall of 1970, I (R.R.) had my first encounter with an electron probe microanalyzer. The “Probe” was in a spacious lab on the third floor of the new Geophysical Sciences building of the University of Chicago. The austerity of the outside design of the building, inspired by the Tuscan town of San Gimignano with its 100 medieval towers, was in

contrast with the modern and rational use of the interior. However, the medieval austerity was preserved in the very narrow, slit-type vertical windows, providing no distraction from the outside world, thus making the scientists concentrate on their indoor activities. My supervisor, Professor Joseph V. Smith, was in charge of the lab, and he personally took me through all the steps involved in obtaining the elemental analysis of silicate minerals from the X-rays generated by a focused electron beam capable of exciting the characteristic lines of each one of the elements present in the sample. The beam could also be made to scan over the sample surface to obtain a secondary electron image similar to that obtained in a scanning electron microscope (SEM) or, alternatively, one could obtain elemental maps by modulating the cathode ray tube (CRT) brightness with the spectrometers’ output. In both cases, a useful image could only be obtained by taking a photographic exposure of the CRT in the slow scan mode. Figure 1 shows the layout of that instrument. Note the absence of any video display.

Besides having worked on the theory and practice of X-ray emission in minerals (e.g., Smith, 1965; Smith & Ribbie, 1966; Rucklidge et al., 1971), Joe Smith’s ability with the actual instrument was exceptional. He could keep in mind all the readings (peaks and backgrounds) of the three spectrometers involved in the analysis of the nine or so elements, and he could drive the spectrometers, two at a time; a hand-crank in each hand (turning both clockwise or anticlockwise, but not always in unison), at such speed as to complete the data collection of each analysis spot in about 10 min! When considering read-out times of 20 s on both, peak and background, it meant that Joe could drive the machine (literally by hand) at the same speed at which it could collect the data! Beam

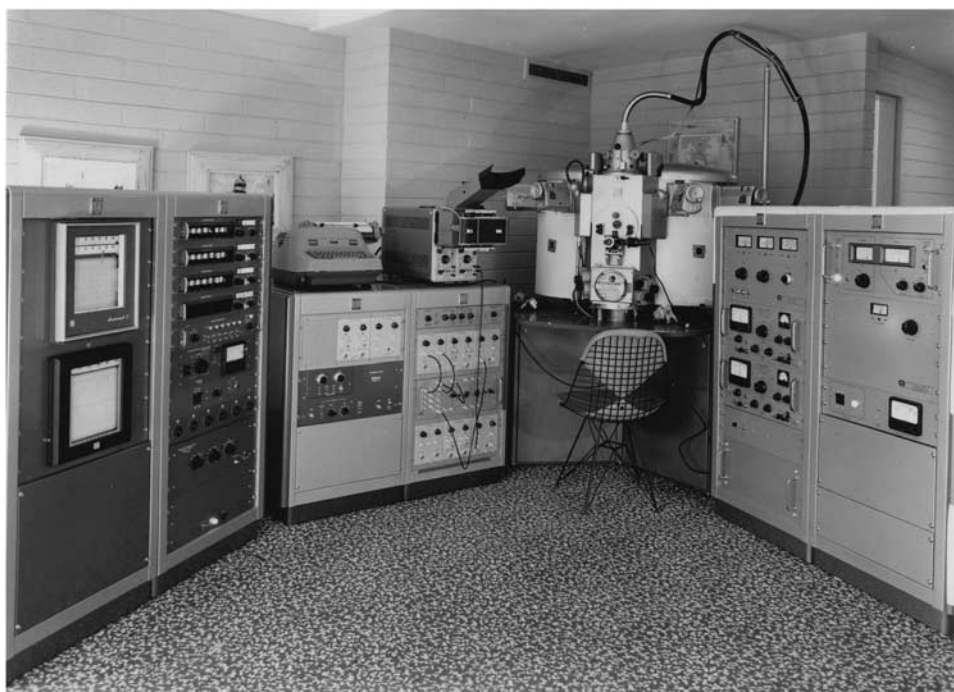


Figure 1. American electron probe microanalysis instrument of the mid-1960s. Note the hand-cranks provided to speed-up spectrometer positioning. The motors were essentially used for peak profile scans (recorded on chart recorders on the left). No computer to control machine functions or data reduction (ARL EMX-SM from David B. Wittry's archives, courtesy of John Fournelle).

blanking and read-out were rhythmically marked by the clatter of the card puncher, and this was the only bit of automation there was. However, what a feat, getting out of that dark and noisy probe room into the crisp Chicago evening air for a walk over to the Computer Center with the loot of punched cards in a long metal box on the way back to the dorm and to then pick up the print-out the next morning on the way back to another analytical session.

Data reduction was then carried out with in-house methods and, later on, with the Bence-Albee method using the newly released Albee and Ray correction factors for binary oxide systems (Albee & Ray, 1970). The lab was soon hooked-up with the main frame via an I/O teletype (TTY) terminal and was heavily involved with the analysis of Moon samples retrieved by the Apollo 11 and 12 missions, along with several other labs in the United States and elsewhere. Stepping motors and automation of spectrometers and stage motions were soon implemented to allow collection of the large data sets needed for such projects.

Upon returning to my Alma Mater, the University of Modena, a few years later (in 1975), I was charged with the responsibility of running the first automated and computer-controlled electron microprobe in Italy, and I dedicated the next 10 years or so to the probe lab and to promoting the self-catering access to EPMA after training colleagues and students from all over Italy (Rinaldi, 1978, 1979, 1980, 1981, 1985).

The moon-shot technological jump had also had its impact on EPMA technology, and a totally new generation of

instruments was in fact fast replacing the “old-timers” of only 5 years before. The instruments were then computer controlled by dedicated hardware and software systems, the heart of which was a Programmable (basic language) Data Processor (PDP-11) with 16×16 -bit bytes of memory (no, not kilobytes and certainly not terabytes!). The hardware (machine) control was accomplished, thanks to the Nuclear Physicists, by their standardized interface system called Computer Automated Measurement and Control (e.g., Kane, 1974). The input-output device was a TTY with a paper tape punch and reader attached. In Figure 2, an image of the instrument in a slightly newer version, when the old TTY was already replaced by a Digital Equipment Corporation printer is shown. A couple of years later, the automation system was retrofitted with a “floppy disk operative system” and a video-terminal (B/W) I/O device (Rinaldi, 1980). By the early to mid-80s, the fast development of computers and electronics in general opened up a world of innovation in electron microprobe analysis, so much so that it became difficult to keep the pace of automation and software development with the existing hardware, still capable of excellent performance as to both wavelength (WDS) and energy (EDS) dispersive systems.

Those were the years when the study of minerals and rocks received an impulse comparable with that caused, some 120 years earlier, by the introduction of the polarizing petrographic microscope for the study of rocks in thin sections. This is also testified by the peak that occurred in the discovery of new minerals. Thanks to the micro-analytical

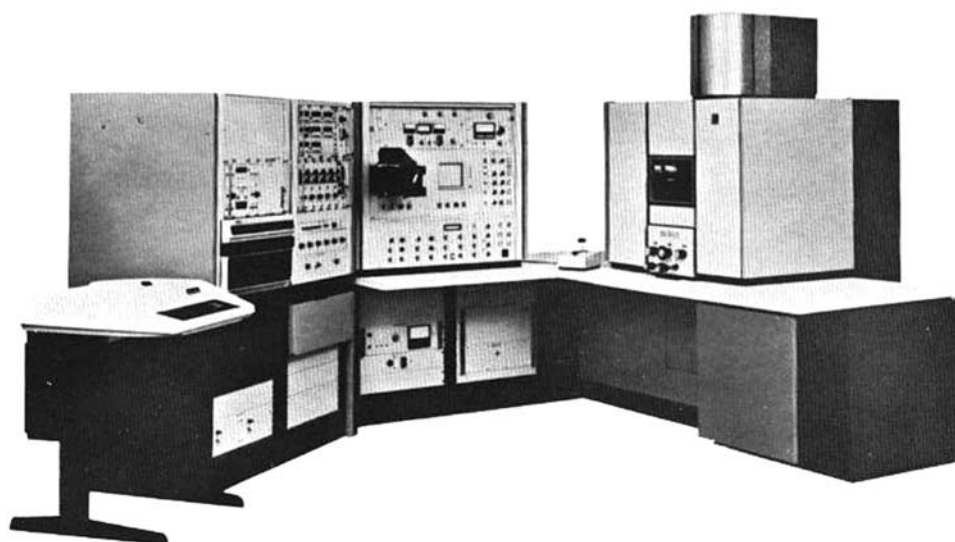


Figure 2. A more modern American microprobe of the mid-1970s (ARL-SEM-Q), at the beginning of computer controlled automaton. Note the Programmable Data Processor of the Digital Equipment Corporation next to the printer. There is no computer video display. Note the dual cathode ray tube screens—one for photos (slow scan) and the other for visual inspection, capable of TV scan mode (courtesy of Fritz Prizivarra).

capabilities, many new phases, generally crystallized as small grains, could be fully characterized. Just looking at my own direct experience, eight new minerals were discovered in those years at my laboratory alone [mazzite, merlinoite, amicitte, saneroite, cascandite, jervisite, katoite, and wakefieldite-(Ce)]. This means that the 300 or so probe labs in Earth Science research establishments around the world increased the number of known natural species of minerals by many hundreds, something like 1/3 more of all species of minerals known until then.

The large throughput of accurate analytical data also made it possible to undertake projects of systematic crystal-chemical studies of complex isomorphic series of rock-forming minerals (feldspars, pyroxenes, amphiboles, spinels, etc.); thereby, vastly extending the knowledge of petrogenetic factors underlying the dynamics of the Earth's interior. The need and desire to find all possible nuances in the very rare and precious moon rock samples induced scientists to undertake very detailed investigations on terrestrial minerals and rocks. This way, the lunar exploration helped discover a large quantity of unknown features related to Earth materials, thus greatly improving the knowledge of our planet. On the other hand, the complexity of natural materials called for ever improved analytical capabilities. Another example of how basic research is the most effective driver of technological development.

More Recent Times

It was during those years, in 1983, that I had the fortune to meet the founding father of the technique, Professor Raymond Castaing. The occasion was the 10th International Congress on X-Ray Optics and Microanalysis in Toulouse, where I happened to sit at his table during dinner.

Raymond was recounting the story of when, during his PhD thesis work, under the supervision of Professor André Guinier some 32 years before (Castaing, 1951), he was faced with great difficulties and a good dose of skepticism while trying to obtain a measurable X-ray signal with Guinier's spectrometer from the primary excitation of a stationary electron beam impinging on a metal sample in an electrostatic transmission electron microscope (TEM) adapted for that purpose. His gut feelings at the time were rather mixed, and he recounted that many times he got totally discouraged. Despite that, he carried on improving the set-up until he managed to make his supervisor (and himself) quite happy in the end. Incidentally, André Guinier was also sitting at that same dinner table and found Raymond's description of those early days quite amusing. After dinner, I had the courage to go up to Professor Guinier and ask for his autograph on the book of abstracts, which he was happy to sign for me; a very fond memory to be recalled in this year, the centennial of X-ray crystallography, of which Guinier had also been one of the leading figures in the early days (Duncumb, 2001; Grillon & Philibert, 2002).

Besides his ingenuity with those rather primitive instruments, Castaing had the great merit to demonstrate the proportionality between the intensity of the emitted X-ray signal and the concentration of the emitting element, once account is taken (by empirical factors) of the nature of the sample (matrix effect). Castaing had actually formulated two approximations, one regarding the proportionality and the other regarding the matrix effects; the combination of these two approximations form the core of what is known as Castaing's Principle—the fundamental law of EPMA. Curiously enough, Castaing's basic principle, together with the use of appropriate standards, is nowadays being re-discovered for the latest quantitative applications of EDS

spectrometry with the latest generation of detectors (Newbury & Ritchie, 2013), despite over 60 years of development in methods for calculating all possible matrix effects from first principles.

At that same Congress, in 1983, several novelties that were to become important stepping stones in the advancement of the technique were presented. With no claim to completeness, I will mention just a few that are still of interest to this day. A new approach to matrix effects for quantitative analysis, the Φ - ρ - z correction, applied to both, bulk and layered samples (Pouchou & Pichoir, 1983a, 1983b), later referred to as the PAP method from the initials of the two authors. The application of Monte Carlo (MC) simulation methods to the analysis (Murata et al., 1983) and thickness determination (Armigliato et al., 1979, 1983) of thin films on substrates. An improved absorption correction (Love et al., 1983) derived by MC fitting of Φ - ρ - z curves covering a wide range of experimental conditions. The latest developments of some of these themes will be treated in the following sections of this paper.

The instrumental complexities and theoretical challenges that Castaing had to overcome initially were only the beginning of a constant challenge that had to be met by people running the instruments that were made commercially available starting in the early 60s and until the mid-70s of the last century. This favored a constant exchange between users and manufactures, which, to this day, enjoy a special kind of symbiosis on the subject, as can be strongly felt during meetings dedicated to the technique and its applications.

It was in this period (early-1960s–mid-1970s) that the analysis of “platinoids” (now platinum group minerals, or PGM), usually occurring as very small grains dispersed in rocks, was undertaken by Professor Eugen F. Stumpfl, a pioneer in EPMA of minerals (Stumpfl, 1961; Stumpfl & Clark, 1965) and the founding father of the lab hosting the 2014 EMAS Workshop from which the collection of papers in this special issue has been derived.

As a matter of fact, the beginning of the use of the electron microprobe for the analysis of minerals and rocks as an established and almost mandatory technique in this field can be traced to around 1964, when some 60 papers were published worldwide, reporting mineralogical analyses obtained by this technique (Keil, 1973). Therefore, we can safely assume that this year (2014) marks the 50th anniversary of the application of the technique in Earth Sciences. The year 1964 also coincides with the first meeting of the Microbeam Analysis Society in the United States of America.

Around the mid to late 1990s (e.g., Rinaldi, 1997), thanks to the huge improvements in microelectronics, automation, and informatics, EPMA tended more and more to become a “black box” routine for a vast number of users, and the general consensus was that it had developed towards a “mature” technology. In other words, not many more improvements could be expected in the medium term, or at least advances at the same rate as during the previous 10 years or so, could no longer be expected. Within only a

few years, this assessment proved to be very wrong as will become clear in the following sections.

THE LATEST DEVELOPMENTS AND THE NEW AGE OF EPMA: A BRIEF OVERVIEW

The constant search for low detection limits and high spatial resolution has recently given EPMA a whole new scope. The idea of trace element analysis, which has been emerging more and more frequently as a favorite issue, is now considered almost common place with the new generation of electron probes with both WDS and EDS spectrometers. The paper on age dating through EPMA of U, Th, and Pb by John Bowles in this issue (Bowles, 2015) is a good example of the possible applications of reliable low and trace element concentration analysis by EPMA. Ultimately, the capability of trace element analysis by electron microprobe has become a reality with present-day instruments and data processing software, reaching well below the 0.1 wt% level and into the parts per million (ppm) range (Jercinovic et al., 2012).

On the other hand, high spatial resolution has always been the specialty of the technique. However, when account is taken of the actual interaction volume which everybody has learned to appreciate from MC simulations at least from a graphical point of view, it becomes quite evident that the search for better resolution is essential, as shown in Figure 3.

Traditionally, pushing the limit of the lowest detection limit with a WDS spectrometer has meant increasing the collection time, as suggested for instance by the classical expression proposed by Ziebold (1967):

$$C_{DL} > 3.29a / (ntP \times P/B)^{1/2}$$

where the limit of detectable concentration (C_{DL}) depends on a factor (a) relating to composition and intensity, on the number of observations (n), and on the counting time (t); and where P is the peak count rate and P/B the peak-to-background ratio.

More advanced statistical expressions have introduced confidence levels and standard deviations on the measurements and considerations on precision and accuracy, depending on the peculiarity of the sample examined, such

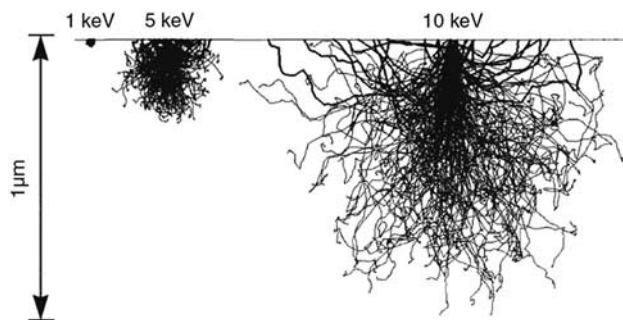


Figure 3. Electron trajectories in Si with $E_0 = 1, 5$, and 10 keV, computed using Monte Carlo simulations. The penetration range of electrons reduces considerably with decreasing beam energy.

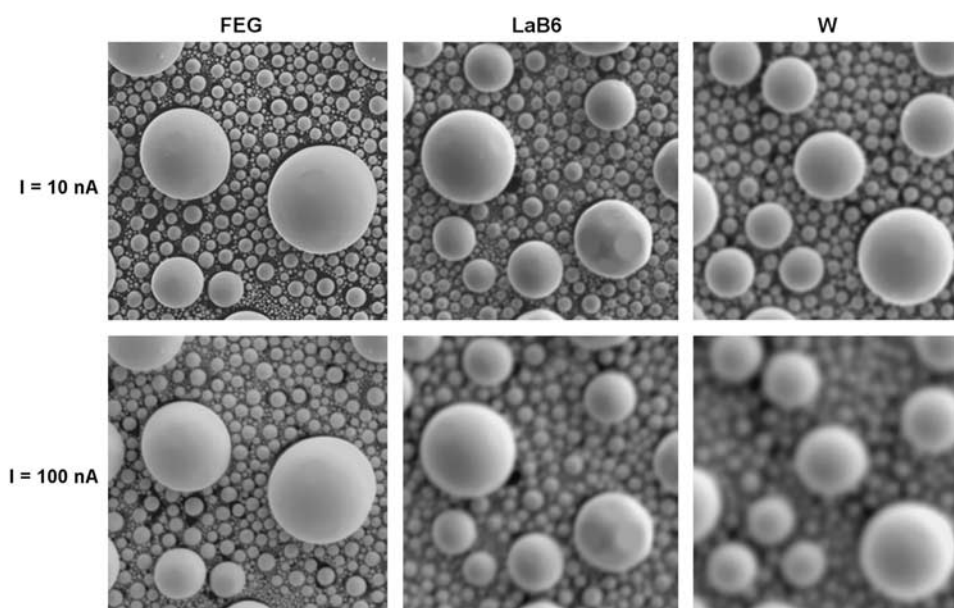


Figure 4. Electron micrographs from Au particles. Left images obtained with a field-emission gun, center with a LaB₆ cathode, and right with a W filament. Top beam current of 10 nA; bottom, 100 nA. Accelerating voltage 10 kV, magnification 5,000× (reproduced with permission of JEOL).

as small particles, sensitive material, etc. (Jercinovic et al., 2012), and taking into account the stochastic nature of the generation.

In any case, the limit is reached when statistical fluctuations due to instabilities intrinsic to the system approach the same level as the signal. The key to improving the detection limit is, therefore, a strong signal with high stability. The latter is clearly where the advancement in fast response (picosecond) electronics comes into play. As to the number of counts produced, this can be improved by a variety of measures that include high reflectivity large crystals, improved vacuum systems, and, last but not least, a new kind of electron emitter making use of the field effect as opposed to the traditional thermionic emission.

The field-emission gun (FEG) is probably the most remarkable of the latest improvements. When compared with a W-filament emitter, its brilliance is several 100-fold better, and stability, once a difficult requirement to be obtained, is no longer a nightmare, thanks to fast electronics. The design in itself is quite simple, the emitter cathode is again tungsten, but in the form of a solid single crystal cone tapered into a very fine point upon which a strong magnetic field extracts the electron beam by a principle as old as that on which the lightning rod was conceived by Benjamin Franklin 265 years ago! As a matter of fact, the theory of field emission kept several eminent physicists busy for a good part of the 20th century until its practical application was finally introduced as a commercial alternative in electron microscopy during this last decade. As is often the case, there are several different designs of FEG's, but their description is beyond the scope of this brief account. It is sufficient to note here that the electron beam produced by an FEG is much smaller in diameter, more coherent, and has a brightness

(current density) almost three orders of magnitude greater than that produced by a conventional thermionic emitter such as a tungsten filament or a lanthanum hexaboride cathode. The result is a great improvement in signal-to-noise ratio, spatial resolution, emitter life, and reliability. Each one of these improvements has a bearing on extending the capabilities of the electron beam instrument as to both image and analysis. The latter being the most important aspect in EPMA. Figure 4 provides a visual comparison of the image resolution obtained with the three kinds of emitters (FEG, LaB₆, and W).

All manufacturers of EPMA instruments and electron microscopes (both SEM and TEM) currently offer the field emission alternative, and this is seen in the names of the instruments that may have an "FE" or an "F" as suffix or prefix. The improved emission from a point source allows sub-micrometer analytical probe sizes (10–80 nm; e.g., Berger & Nissen, 2014), again an improvement of three orders of magnitude over a traditional emitter. When combined with low voltage operation (5–7 kV), this results in a very shallow penetration depth, and therefore a dramatic reduction of the analytical volume (volume of interaction, as shown in Fig. 3), and a generated signal (thanks to the high brilliance), which is still strong enough to provide full analytical capabilities for both spectroscopies (WDS and EDS).

Although the negative trade-offs for low voltage operation may require special care and a whole new approach for quantitative analysis (Merlet & Llovet, 2012; Pinard & Richter, 2014), the advantage of a greatly reduced interaction volume opens up a large variety of new applications in the characterization of thin films and nanomaterials. The pros and cons of these new avenues offered by the FEG in EPMA are discussed in more detail in the Analytical Capabilities Today: Advantages and Disadvantages section.

Another instrumental development has recently provided great improvement in EDS with the introduction, during the last decade, of a new device—the silicon drift detector (SDD)—the development of which has been as fast as to have already reached its 6th generation. When compared with the traditional lithium drifted silicon detector (Si (Li) detector), this new kind of device, although working on exactly the same principle, provides a considerable number of advantages. The first and the most noticeable, even to the untrained eye, is the lack of the cumbersome and inconvenient liquid nitrogen cryostat and the reduction in maintenance activity this implies. The detector can in fact operate at room temperature or with moderate cooling, such as that provided by the thermoelectric (Peltier) effect, thanks to the very low leakage current generated within the device. The other main advantage is the count rate performance, which is up to two orders of magnitude greater than that of a Si(Li) detector (Newbury & Ritchie, 2013). All this, combined with an energy resolution close to the theoretical value of 120 eV for a silicon device, makes the SDD a desirable analytical tool for all kinds of electron microscopy. A comparison of performance between EDS and WDS spectroscopies now has to take into account the great improvements one can obtain with this latest generation of solid-state detectors where a definite advantage can be scored, for instance, in the acquisition speed of X-ray maps. However, when energy resolution and low detection limits are at stake, WDS detectors remain as the technique of choice for quantitative analysis, especially for trace and light elements (Maniguet et al., 2012).

In the field of WDS spectroscopy, a very recently introduced device provides considerable improvement in the analysis of very soft X-rays, including Li and Be among the elements that can be quantitatively analyzed. This type of spectrometer makes use of a new grazing incidence grating technology, whereby dispersion of the incident X-rays is obtained by Bragg reflection over a physical grating rather than a crystal lattice. The combination of a laminar-type varied-line-spaced (VLS) grating with a high-sensitivity X-ray CCD detector allows simultaneous collection of a full spectrum (within a limited wavelength range), thus making the device somewhat comparable with EDS. Having been introduced only very recently, testing of the device is still limited to a few emblematic examples that have been provided by the manufacturers. However, there is no reason to doubt the promise to considerably expand the capabilities of EPMA, as discussed in more detail in the last section dealing with the envisaged future.

Most, if not all, of the above-mentioned advances are extending the limits of EPMA toward higher spatial resolution and lower detection limits. The trade-off is normally the increasing importance of some adverse effects that the analyst has to take into account. Among these effects, a few are worth mentioning here even if they will not be discussed in detail according to the nature of this brief review. Carbon contamination and sample “damage” by the electron beam both merit attention here. The latter comprises effects such as migration of elements from the analytical volume, also in

response to different crystal orientations of the sample (and reference standard) under the beam. Some of these have recently been reviewed (Donovan, 2011). The usual strategies to avert or limit these effects include the careful choice of instrumental parameters, the use of an anti-contamination device and/or of a cryostage, careful monitoring of the effects, and use of empirical correction coefficients as a function of dwell time.

Other caveats, especially when working with low-energy lines (low voltage excitation), include the need to revisit the mass attenuation coefficients (MACs) (e.g., Gopon et al., 2013) and the effects due to secondary fluorescence (SF) at grain boundaries (e.g., Llovet et al., 2012; Wade & Wood, 2012). Some of these aspects are treated in more detail in the following section, with a few examples of applications.

ANALYTICAL CAPABILITIES TODAY: ADVANTAGES AND DISADVANTAGES

Improved Detection Limits for Trace Analysis

Use of electron microprobes for trace element analysis has increased over the years, mainly because of the improved stability of electron columns operated at high-beam currents and the development of new crystal analyzers with larger areas. Figure 5 provides a comparison between these newly

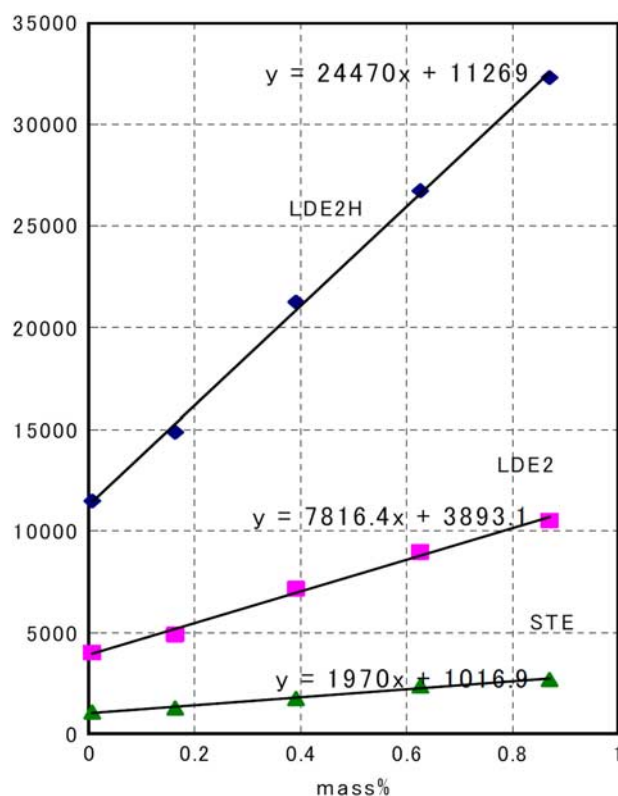


Figure 5. Sensitivity of newly developed LDE2 and LDE2H crystals, as compared with traditional STE, for the analysis of C. Detection limits are 12 (LDE2H), 23 (LDE2), and 49 ppm (STE) (after Mori et al., 2011). Reproduced with the permission of JEOL.

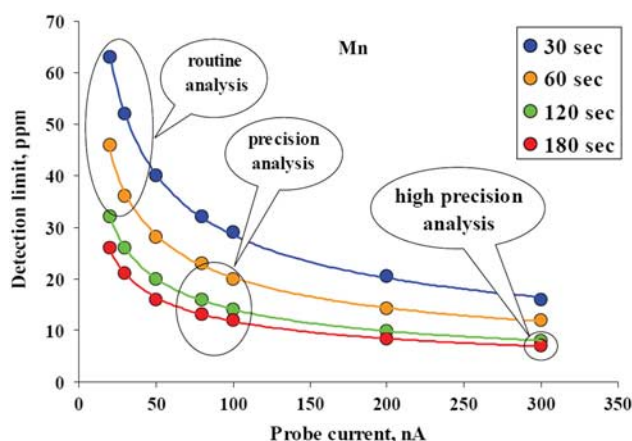


Figure 6. Detection limit for Mn in a San Carlos olivine standard as a function of probe current and peak counting time. Typical conditions for routine, precision, and high-precision analysis are marked (after Sobolev et al., 2007). Reprinted with permission from AAAS.

developed crystals and the traditional one (STE) in C analysis. These developments have made it possible to decrease the detection limits of the technique down to a few ppm by simply using high-beam currents (up to 3 μ A) and long acquisition times. Figure 6 shows an example of the detection limits achievable by using this analytical strategy.

However, one should bear in mind that the accuracy of EPMA decreases at low concentrations, essentially because most sources of random and systematic errors are magnified (Jercinovic et al., 2012). The most important sources of errors are spectral background subtraction, beam damage, SF from phase boundaries, carbon contamination, and, to a lesser extent, instrumental instability.

The conventional method of background subtraction by linear interpolation of two measurements on each side of the peak may lead to unacceptable errors for trace elements due to the curvature of the background and/or to the presence of tails of peaks from other elements. Detailed wavelength scans around the peak of interest are essential to assess the reliability of background subtraction, as well as tests on blank standards that do not contain the element of interest (Reed, 2000). Interestingly enough, predigital instruments were invariably equipped with analog chart recorders and plotters (see Fig. 1) for the purpose of peak profile studies.

Merlet & Bodinier (1990) proposed an improved method for background subtraction that consists of least-square fitting of several background measurements performed on different channels to a background model based on a modified form of Kramer's equation. Another possible solution is to use a calibration curve, which must be obtained on reference samples having similar composition to the sample of interest. In this case, a background subtraction is not required, and conversion of intensity to concentration is carried out directly from the measured intensities. This is the basis of the analysis of, e.g., C and N in steels (see e.g., Moreno et al. 2002).

Instrumental and sample stability during long acquisition times can be monitored by means of statistical tests (e.g., χ^2 test along with Dixon and Grubbs filters), as discussed by Merlet & Bodinier (1990). This procedure requires the long counting times to be divided into many short counting times and alternating peak and background measurements to minimize instrumental drift.

The problem of SF across phase boundaries arises from the fact that characteristic X-rays and bremsstrahlung produced by primary electrons can ionize atoms at much larger distances from the point of impact than primary electrons. Indeed, although the range of primary electrons is of the order of a few micrometers, that of the generated characteristic and bremsstrahlung X-rays can be one-to-two orders of magnitude larger. This means that, even for electron beams impacting quite a distance from a phase boundary, there can be a fluorescence contribution arising from the neighboring phase. This contribution is important for trace analysis, especially when the neighboring phase contains an appreciable concentration of the element of interest. This effect will be discussed in more detail in the Limitations and Problems subsection.

Examples of improved methods for the analysis of trace elements include those developed by Merlet & Bodinier (1990) and Fialin et al. (1999). The latter authors developed a procedure to improve the detection limits as well as the precision and accuracy of trace analysis that includes fractional counting times at several sample positions (to mitigate sample damage), statistical data filtering, and improved background modeling. The capability of the method developed was demonstrated by analyzing glass samples spanning different compositions yielding detection limits of 6–8 ppm for Cr and Ni, 23 ppm for Y, Zr, and Sr, 15 ppm for RE elements, and 35 ppm for Pb and Th. The analyses were performed at 35 keV, 500 nA, and total counting times of 15 min. Jercinovic et al. (Jercinovic & Williams, 2005; Jercinovic et al., 2008, 2012) examined factors affecting the accuracy of trace analysis in accessory minerals such as monazite, found in multiphase geological materials, for which not only high sensitivity but also high spatial resolution is required.

To assess the accuracy of the results, it is common practice to rely on comparisons with other micro-analytical techniques such as particle-induced X-ray emission (PIXE) or laser ablation inductively coupled mass spectrometry (LA-ICP-MS). This is the case, e.g. of Sobolev et al. (2007), who used systematically high-current EPMA for the analysis of trace elements in olivine to investigate the geo-chemistry of the sources of mantle melts. These authors analyzed >17,000 olivine grains and reported detection limits of 6–15 ppm and errors of 15–30 ppm (at 2σ level) for the elements Ni, Ca, Mn, Cr, Co, and Al in this mineral. Reproducibility and accuracy of the EPMA results for this particular mineral were satisfactorily assessed by comparison with LA-ICP-MS results.

Low Voltage and High Spatial Resolution

The incorporation of FEG technology in the SEM and, more recently, in the electron microprobe (Kimura et al., 2006) has

stimulated the operation of these instruments at low voltage. An FEG electron source yields a finely focused (<100 nm) electron beam with relatively high current (up to 100 nA) even at low beam energies (<5 keV). At such energies, the effective ionization range of incident electrons drops from the conventional micrometer scale down to the sub-micrometer scale and leads to significant improvement in the lateral resolution and surface sensitivity of the technique (Barkshire et al., 2000; Newbury, 2002; Merlet & Llovet, 2012).

The effective ionization range of electrons R can be calculated at first approximation using a simple formula proposed by Castaing (1951):

$$R = \frac{33 \times A}{\rho Z} (E_0^{1.7} - E_i^{1.7}) \text{ nm}$$

where E_0 is the incident electron energy (expressed in keV), E_i the ionization energy of the considered shell (in keV), A the atomic weight, Z the atomic number, and ρ the density (in g/cm³). As an example, the effective ionization range of 20 keV electrons incident on a light matrix such as C ($Z = 6$) to excite Fe $K\alpha$ X-rays is 3.9 μm , whereas it drops down to 123 nm for 2.5 keV electrons in the excitation of Fe $L\alpha$ X-rays. A more accurate estimate of the ionization range requires knowledge of the electron beam size (Pinard & Richter, 2014). These authors have developed a procedure to find the optimal analytical conditions to achieve the best spatial resolution.

The use of FEG-EPMA at low voltage has opened new possibilities for the characterization of complex materials that are heterogenous on a sub-micrometer scale. Examples include the analysis of small crystals or inclusions, exsolution lamellae, fine-scale mineral intergrowths, reaction rims, complex zoning patterns, slow diffusion processes, etc. An example of the application for the characterization of exsolution lamellae is given in Figure 7.

However, EPMA at low energies is marred by experimental and analytical problems that affect the accuracy of quantitative results and require new analytical strategies (Willich & Bethke, 1996; Merlet & Llovet, 2012; McSwiggen, 2014). First of all, the less intense, low-energy X-ray lines (mostly L- and M-lines) have to be used, which are often affected by peak shifts, peak overlaps, and larger uncertainties in the MACs. In addition, for the L- and M-lines, the fluorescence yields are generally lower than those for the conventional K-lines. As a result, peak-to-background ratios are also lower and the detection limit worsens. Duncumb & Statham (2002) have shown the benefits of using X-ray spectrum simulations for the interpretation of EDS X-ray spectra at low energies, where on top of the mentioned effects there are the problems of a sloping background and a large change of detector efficiency.

In the case of the transition elements, both the emission and absorption of X-rays are still poorly understood when they originate from electron transitions involving the partially filled 3d shell (Pouchou, 1996). This is the case, e.g. for the most intense and widely used $L\alpha$ (transition M5-L3) and $L\beta$ (transition M4-L2) lines. The strong limitation of the use

of $L\alpha$ and $L\beta$ lines for routine analysis of transition elements has been discussed recently in a round robin study (Llovet et al., 2012), where the participants analyzed a monophasic alloy steel sample at low voltage (5–6 keV). The results showed an underestimation of the Cr contents, with relative deviations from the reference values ranging from –0.7 to –17%, and an overestimation of Fe and Ni, with relative deviations from the reference composition ranging from –4 to +30% and from +14 to +42%, respectively. An example of such deviation is given in Figure 8. More recently, Jonnard et al. (2014) reported the results of another round robin study, where the participants analyzed a metallic glass sample. The results obtained at 5 keV showed an overestimation of the Ni and Co contents by 13 and 11%, respectively.

To overcome this limitation, Gopon et al. (2013) suggested the use of other L-lines such as the less-intense L1 line (transition M1-L3). The latter authors have shown that using such an X-ray line, which does not involve transitions from the unfilled 3d shells, yields reliable results for Fe silicides. Nevertheless, use of the less-intense L-lines has practical limitations, and therefore efforts are currently being directed towards understanding the $L\alpha$ and $L\beta$ anomalies. Of course, this problem can be mitigated by using standards of similar composition to the unknowns, as shown by Ohnuma et al. (2012) in a study of the Fe–Si binary system, where analyses were performed at 6 keV using a FEG-EPMA and a homogenous Fe–Si alloy as a standard.

An alternative to using the L-lines excited at low voltage is to use K-lines excited at low over-voltages—i.e., with an incident electron beam energy of only a few keV above the ionization threshold. The effective ionization range can still be suitable for some K-lines to analyze sub-micrometer features, as pointed out by McSwiggen et al. (2014). The main problem for the analysis at low over-voltage is the low count rates and peak-to-background ratios, which increase errors and detection limits and require long counting times. McSwiggen et al. (2014) have suggested the use of different accelerating voltages for different elements to optimize the analysis of sub-micrometer features, in a similar way as carried out for the analysis of thin films and multilayers (Llovet & Merlet, 2010). For selected elements, EDS analysis of K-lines at a low over-voltage is an alternative strategy for improving spatial resolution that could give higher accuracy (Statham & Holland, 2014).

At low-beam voltages, a surface layer several nanometers thick represents a much larger fraction of the sample, and therefore the influence on the accuracy of the analysis results of carbon contamination, surface oxidation, the quality of the sample polish, or thickness of the conductive coating become more significant. The effect of carbon contamination on the analysis of carbon-coated silicate minerals at 5 keV has been examined by Buse and Kearns (2014). They concluded that carbon contamination becomes important for closely spaced analyses, where each analysis point overlaps the carbon contamination ring produced by the previous analysis spot, and have developed an empirical

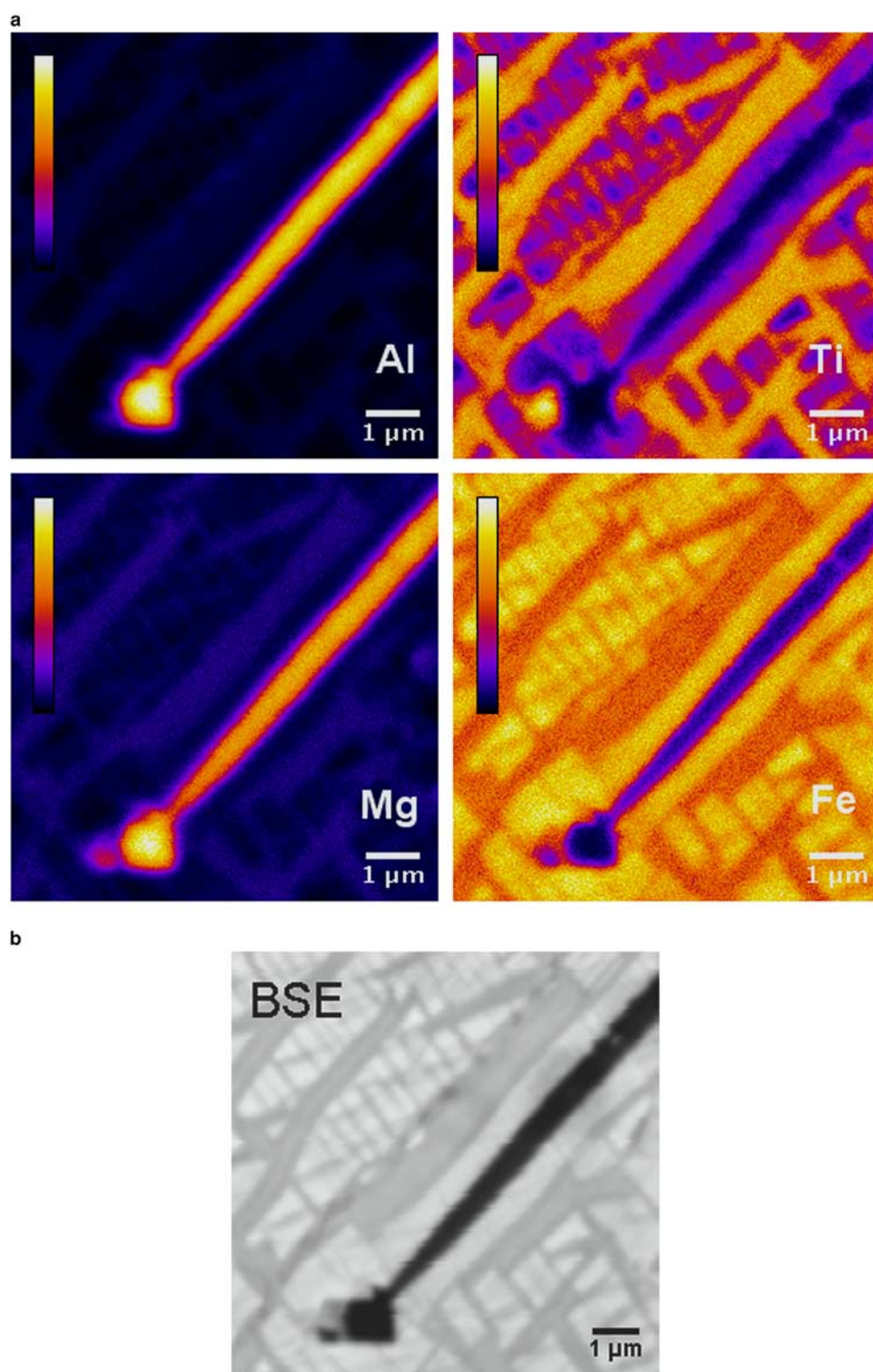


Figure 7. X-ray maps for the distribution of Al, Mg, Ti, and Fe and backscattered electron (BSE) image of a sample consisting of exsolutions of ilmenite and ulvöspinel in Ti-magnetite, obtained using a JEOL 8500F field-emission gun electron probe microanalyser*. Magnification 10,000 \times , beam voltage 10 keV, and beam current 50 nA. Sample kindly provided by Cristina Villanova.

correction to minimize its effect. As mentioned previously, the use of anti-contamination devices such as a liquid N₂ cold finger and/or the recently introduced radio-frequency (RF) plasma cleaner may become mandatory. Figure 9 shows an RF plasma cleaner attached to the prechamber of a

state-of-the-art electron microprobe. Mounting the device in the prechamber of the microprobe prevents interference with the detectors without compromising its effectiveness.

Unfortunately, there is a lack of systematic studies in which the performance of experimental methods and

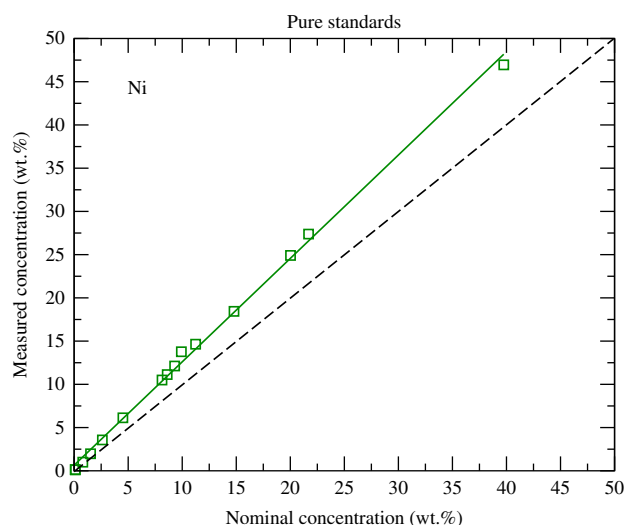


Figure 8. Measured versus reference concentration for Ni in a series of 15 alloy steel samples with varying Ni concentrations. Symbols are experimental measurements. Straight lines represent the results of linear regression. EPMA analyses were performed at an accelerating voltage of 6 kV, using the Ni $L\alpha$ line and a pure Ni standard. The difference between the measured and the reference concentration increases with increasing concentration (after Llovet et al., 2012).

correction algorithms are assessed at low voltage. Such evaluations are needed in order to refine available methods. Because of this, FEG-EPMA instruments are usually used at conventional high energies (15–20 keV) or for imaging purposes, and only few studies can be found in the literature where quantitative EPMA analyses at low voltage are reported.

Improved Data Reductions for Analytical Procedures

The ZAF and α -factor methods have been at the core of quantitative EPMA data reduction programs for many decades. As we have seen in the Brief History from a Personal Perspective section, these first-generation methods were developed in the years following Castaing's pioneering work—e.g., in the 1960s and 1970s. A second generation of matrix-correction procedures, based on the use of the depth-distribution of X-ray production, was developed in the 1980s and in the beginning of the 1990s. These procedures improved the analysis of light elements and allowed for analysis of thin films and multilayers with thickness in the sub-micrometer range (see below). A detailed review of the different correction methods of these second-generation methods was published by Lavrent'ev et al. (2004).

In the 2000s, the development of matrix-correction procedures almost ceased, with a few exceptions such as the extension to nonperpendicular incidence (Bastin et al., 2001) or alternative methods such as those developed by Horny et al. (2010). Nevertheless, and as a result of the extensive research performed over the years, a large number of correction procedures that include different combinations of

physical parameters are currently available in software packages of various commercial manufacturers. However, it remains unclear as to which correction procedure should be used for each specific type of sample, and thus the choice of standards remains critical.

Another area of development corresponds to the so-called standardless analysis, which is useful when standards are not available or simply to shorten analysis time. These developments have been mostly performed by commercial manufacturers (for both EDS and WDS), with few exceptions. Because of that, these methods often use unpublished algorithms whose accuracy is difficult to assess. One of the few exceptions is the method developed by Limandri et al. (2012), which minimizes the differences between a measured spectrum and an analytical function by optimizing parameters involved in the analytical prediction. This is a profile-fitting procedure somewhat similar, in principle, to the widely used methods in X-ray crystallography.

Recently, Trincavelli et al. (2014) reviewed the key features of the most important standardless methods available today, as well as the level of accuracy that can be achieved. They pointed out the danger of using methods that normalize the calculated concentrations to 100%, unless an estimate of the errors is reported. Ritchie et al. (2012) demonstrated that a carefully performed and analyzed EDS measurement can produce results that are as accurate and precise as carefully performed WDS analyses, with equivalent or less time and effort. More recently, Newbury & Ritchie (2013) concluded that SEM/EDS can match WDS in accuracy and precision provided the K -ratio protocol is followed with the use of appropriate reference standards.

Marinenko & Leigh (2010) have shown how to apply the ISO/GUM guide for the evaluation of measurement uncertainties in EPMA quantification. More recently, Ritchie & Newbury (2012) included uncertainty in the MACs and in the backscatter coefficient in the EPMA uncertainty budget, which generally only includes the precision from counting statistics. Unfortunately, these developments have not yet been implemented in the software provided by microprobe manufacturers, and thus have not found application in analytical practice. Another area of development is that of X-ray mapping and postprocessing methods, which aim to discriminate and identify the distribution of most phases present in complex materials (Wuhrer et al., 2006; Pownceby et al., 2007; Prêt et al., 2010).

As mentioned earlier, the second generation of matrix-correction procedures based on the use of depth-distribution of X-ray production allowed their extension to the analysis of thin films and multilayers in a systematic way, and the so-called thin-film programs became available (see e.g., Pouchou & Pichoir, 1993). Because of these developments, EPMA has proven to be a versatile tool for thin-film characterization, supplementing the information obtained from conventional surface-analytical techniques and also providing complementary information about the lateral variation in thickness and composition of thin films at the micrometer scale.



Figure 9. Modern electron microprobe instrument (JEOL JXA-8230)* equipped with a radio-frequency plasma cleaner mounted in the prechamber.

For thin films and multilayers, K -ratios are generally measured for elements present in the different layers at two or more electron incident energies, and the resulting system of equations is solved using iterative methods. By doing so, values of the layer compositions and thicknesses yielding K -ratios that best match the experimental measurements are obtained. As an example, Figure 10 shows the variation of measured K -ratios against electron beam energy, together with the best fit obtained using the thin-film program STRATAGEM (Pouchou, 2002) for an Au/Cu-Zn/Ni/Fe multilayer film. The fit resulting from the use of the STRATAGEM program showed that the sample consists of a 21 nm layer of Au, a 71 nm layer of Cu 67 wt%, Zn 33 wt%, and a 508 nm layer of Ni on a Fe substrate. This model agrees reasonably well with the measured K -ratios as shown in Figure 11.

In recent years, some studies have been devoted to refining existing thin-film programs (e.g., Llovet & Merlet, 2010) and/or to provide systematic experimental measurements (e.g., Bastin & Heijligers, 2000a, 2000b; Merlet et al., 2004) that will be useful for the assessment of the reliability

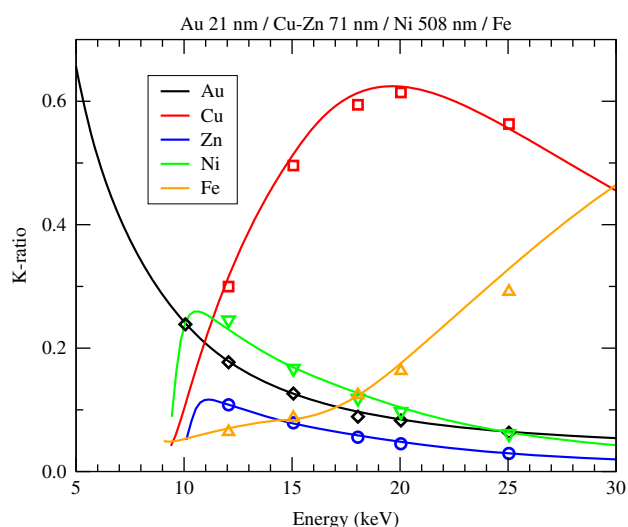


Figure 10. Comparison between calculated and measured K -ratios for an Au/Cu-Zn/Ni/Fe multilayer film. Symbols represent experimental data, and continuous lines are results from STRATAGEM. See text for details.

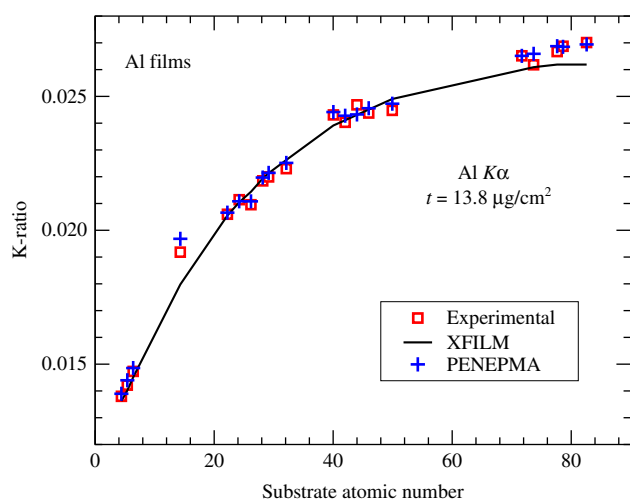


Figure 11. Measured, calculated, and simulated K -ratios for Al films deposited on different substrates versus substrate atomic number. Measurements were taken from Bastin and Heijligers (2000a and 2000b); calculations were performed with the program X-FILM; simulations with PENEPMA. See text for details.

of thin-film programs or MC simulation results (Statham et al., 2014). As an example of the usefulness of such experimental data, Figure 11 shows a comparison between calculated, simulated, and experimental Al K -ratios emitted from Al films deposited on a wide variety of substrates (20 of them). The experimental data were taken from Bastin and Heijligers's database (2000a and 2000b). The K -ratios were calculated analytically with the program X-FILM (Llovet & Merlet, 2010) and simulated using the MC PENEPMA program (Llovet et al., 2005). Some discrepancies can be observed between measured and calculated K -ratios for film-substrate combinations such as Al/Si, which are in part attributed to inaccuracies in the fluorescence correction implemented in X-FILM. The results from PENEPMA provide a much better match for the measured K -ratios.

Limitations and Problems

One of the limitations of currently available correction procedures is due to the assumption that the sample volume from which X-rays are generated is chemically homogenous. As discussed earlier, thin-film programs can be used for the analysis of layered samples. In the case of other inhomogeneous samples such as small particles, inclusions, lamellae, or in general when the legitimacy of the approximations involved in matrix corrections procedures is not firmly established, the MC simulation method has proven to be a valuable tool as a foundation of quantitative procedures.

The first MC simulations of electron transport and X-ray generation were performed at the beginning of the 1960s. These early MC calculations used approximate analytical interaction models and considered only simple geometries to cope with the limited computation power available at that time. Because of this, the use of MC simulation in EPMA was mostly limited to checking the reliability

of correction methods or to guiding the development of improved algorithms. Today, we can use much more reliable electron interaction models, frequently described by means of extensive numerical databases calculated from state-of-the-art theories (see e.g., Salvat et al., 2011). One such example is the recent database of the inner shell ionization cross-sections released by NIST (Llovet et al., 2014a, 2014b). The transport of photons can also be simulated from the corresponding differential cross-sections, thus providing a faithful picture of the whole process, irrespective of the geometrical complexity of the sample. This, together with the increasing availability of faster computers, has allowed MC simulation to become a practical quantitative tool, especially for the analysis of inhomogeneous samples, as shown for porous samples (Sorbier et al., 2004), small inclusions (Pistorius & Verma, 2011), or individual particles (Ro et al., 2003; Chöel et al., 2007).

With the aim of facilitating its application to EPMA, different MC simulation programs have been developed in recent years, which have different capabilities and degrees of sophistication. These include, e.g. the programs CASINO (Drouin et al., 2007), DTSA-II (Ritchie, 2005), Win X-Ray (Gauvin et al., 2006), or PENEPMA (Llovet et al., 2005). The last program uses the general purpose MC code PENELOPE (Salvat et al., 2011).

Another limitation of the technique is the spread of the incident electron beam within the specimen, which sets the limit to the lateral resolution that can be achieved (i.e., the smallest distance between two regions from which independent analyses can be obtained). In diffusion studies, elemental concentration profiles are typically measured by step-scanning along the diffusion direction (i.e., perpendicular to the interface of the diffusion couple). Because of the spread of the electron beam, the composition that is actually measured corresponds to the "spatial" average of the sample composition around the electron beam point of impact. Methods to recover the "true" composition profile have been developed by several authors. Worth mentioning here is the work of Ganguly et al. (1988). These authors developed a method that consists of convolving hypothetical profiles with a Gaussian distribution until a match is found with the measured profile.

As mentioned before, EPMA measurements can be affected by SF effects across the interface boundary, which can lead to unacceptable analytical errors in the case of trace element analysis. The SF contribution depends on the impact distance of the electron beam from the boundary (it increases as the electron beam approaches an interface) and on the shape and composition of the two adjacent phases, and may become significant when the neighboring phase contains detectable concentrations of the element of interest.

The problem of SF near phase boundaries was recognized by Reed & Long (1963), and has been discussed extensively in the literature (see e.g., Bastin et al., 1983). The contribution of SF can be minimized using L- and M-lines instead of K-lines in the quantitative procedure. However, measurement and quantification using L- and M-lines are

difficult and may be affected by even larger uncertainties as discussed previously. Llovet & Galan (2003) used the MC simulation program PENELOPE to correct for SF effects encountered in the EPMA analysis of olivine–clinopyroxene couples for geothermobarometry applications. They also assessed the reliability of PENELOPE for the simulation of SF profiles by comparing simulated “apparent” concentration profiles with EPMA measurements from a series of well-characterized mineral couples. Because PENELOPE simulates both the electron and photon transport, the contribution of SF from characteristic X-rays, as well as that from bremsstrahlung photons, is considered.

MC simulation can also be used to calculate SF effects in samples with other geometries such as particles or small phases (Myklebust & Newbury, 1995; Llovet et al., 2000). Wade & Wood (2012) used PENELOPE to simulate SF effects for samples from high-pressure metal–silicate partitioning experiments, which consist of small ($50\ \mu\text{m}$) balls of metal embedded in a silicate matrix. Analysis of the silicate was found to be significantly contaminated by SF effects, which led to an underestimation of the partitioning coefficient (in the case of the partitioning of Ni between Ni-rich metal and Ni-poor silicate) of about 25%. Because of that, these authors recommend that every representative experiment be simulated in order to check the possible errors due to SF.

More recently, Llovet et al. (2012) developed a semi-analytical method for computation of the SF contribution across the boundary of two adjacent materials. The method was implemented in a computer code named FANAL, which is publicly available. Using FANAL, SF intensities are calculated numerically by integrating the equations that describe the emission of X-ray fluorescence from two materials when the electron beam impacts on one of them. The calculation makes use of the intensities of primary photons generated from short PENELOPE runs. FANAL includes the contribution from both characteristic X-rays and bremsstrahlung and can be applied to multicomponent materials. Figure 12 shows the results of such a study for a pair of minerals often present in close association in igneous rocks.

A LOOK INTO THE FUTURE

The recent introduction of a new WDS spectrometer produced, up to now, by only one of the two main EPMA manufacturers under the name of soft X-ray emission spectrometer (SXES) has opened a whole new perspective for the analysis of light elements and low-energy lines of other elements (Takahashi et al., 2014a, 2014b). The range of wavelengths explored is necessarily limited to the long, low-energy ones, at least in this first device. The SXES uses a VLS grazing incidence grating to disperse the X-rays, which are then collected by a CCD camera acting as the detector. X-rays with energies in the 50–210 eV range are, thus, detected and quantified. The performance is quite remarkable with, e.g., a sensitivity of a few 10s of ppm for boron in steel. Furthermore, it has now become possible to directly

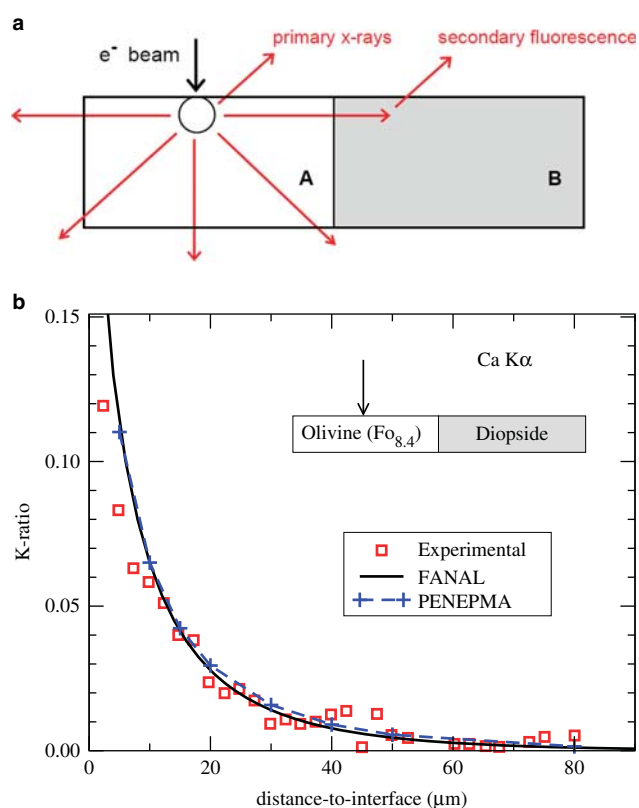


Figure 12. Secondary fluorescence at a phase boundary. Comparison of measured, calculated, and simulated Ca K-ratios for a mineral couple of olivine (8.4% Forsterite, 91.6% Fayalite) diopside (CaMg pyroxene), electron beam impinging on the olivine side. Calculations were performed with the program FANAL; simulations with PENEPEMA (Llovet et al., 2012).

measure the Li $K\alpha$ line (52 eV) and the L-lines of Al (70 eV) and Si (100 eV) using a commercial instrument. SXES is also a sensitive tool for chemical analysis (Terauchi et al., 2014), mainly because of its excellent energy resolution (0.2 eV at the Al L-line), and the fact that most of the measured X-ray lines involve electron transitions from the valence band, which carry information about the chemical state. Proof of this is given by the Li peak in metallic Li, which appears as a well-defined single K-line, whereas in Li-compounds (e.g., LiF, etc.) an additional satellite peak occurs in response to the occupancy of the valence band as shown in Figure 13.

Rapid advances in computer memory and processing power have had and will continue to have a large impact on EPMA. The recent release by a third manufacturer, mostly devoted to the production of instruments for the industrial market, of a totally automated FEG-EPMA, testifies to the revival and further spreading of the technique, thanks to the high level of computer control, achieved through computer codes of the latest generation. All machine functions, even the most trivial mechanical movements have been automated, thereby making the operation of such a complex instrument somewhat similar to that of a smart phone.

Refinement of correction procedures awaits much future work, especially at low voltage and overvoltage,

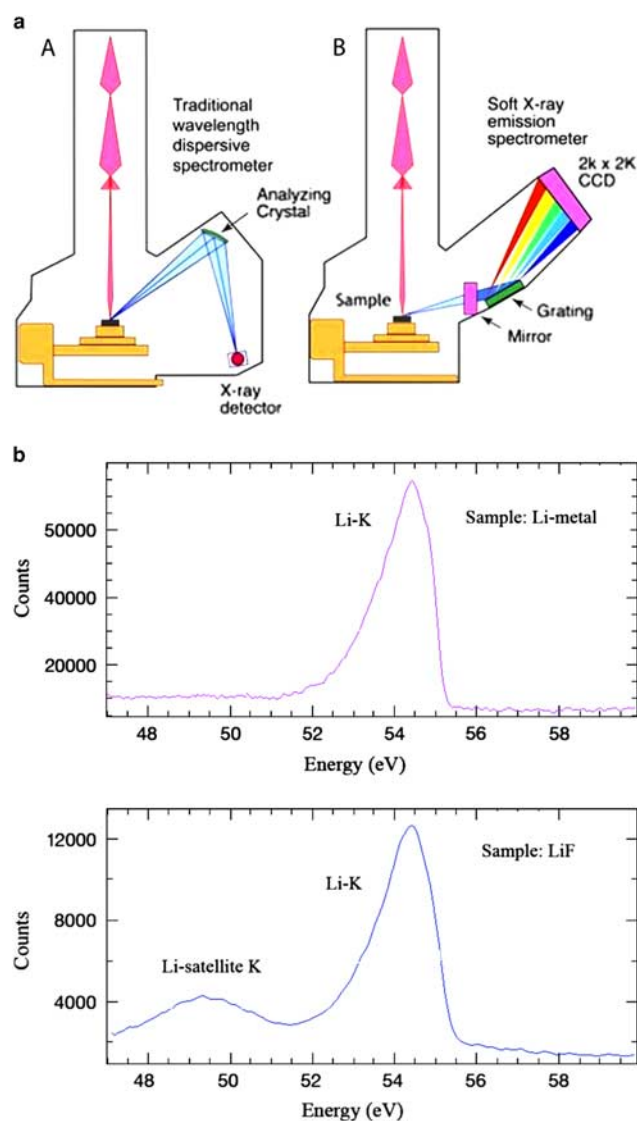


Figure 13. Top: Schematics of soft X-ray emission spectrometer and a traditional wavelength dispersive systems spectrometer. Bottom: Li analysis on pure element and LiF (from Takahashi et al., 2014a). Reproduced with the permission of JEOL.

improving the present situation for the L-lines of transition elements and the M-lines of rare earth elements, and incorporating the N-lines of heavy elements. However, it will also be necessary to perform more and highly accurate K-ratio measurements in order to support such refinements. In the case of thin films, questions still remain about the accuracy of thin-film programs when there is a large difference in atomic number between adjacent layers. On the other hand, MC simulations are likely to continue to develop with respect to accuracy and user friendliness, and will probably form the basis of a third generation of correction procedures directly available at the instrument console.

The use of multiple accelerating voltages in more fully automated instruments is also likely to continue to develop for the characterization of complex material samples. Future goals of EPMA will include the simultaneous collection of

EDS, WDS, SXES, EBSD, and cathodoluminescence signals. These multispectral data sets will provide detailed chemical and structural information of complex materials at high spatial resolution (MacRae et al., 2014). The problem of accurate elemental analysis in tilted samples of small heterogeneous inclusions investigated by EBSD, has to be addressed. Another area of development will probably be the combined use of the focused ion beam (FIB) and the FEG-EPMA. Indeed, by FIB thinning the samples and analyzing them at high voltages using a FEG-EPMA, Kubo et al. (2013) demonstrated a spatial resolution in the range 40–200 nm for an InGaP/GaAs thin sample, with detection limits of 1,000–10,000 ppm and signal-to-noise ratio 13 times higher than that of a STEM-EDS system (on bulk samples such detection limits would be 2 to 3 orders of magnitude lower). Worth mentioning is also the development of three-dimensional microanalysis in dual-beam instruments (i.e., SEM equipped with both EDS and FIB), which will require more sophisticated quantification methods such as the one recently developed by Burdet et al. (2014).

In conclusion, EPMA is still a very lively technique, with a wide range of applications in all avenues of material science and the prospect of many further developments in the technique itself and its applications.

ACKNOWLEDGMENTS

The authors thank the European Microbeam Analysis Society for support for participation in the EMAS-2014 Workshop in Leoben, Austria. Financial support from the Spanish Ministerio de Economía y Competitividad, project no. FPA2013-44549-P is gratefully acknowledged. Thanks are due to John Fournelle for the picture of Fig. 1 (from the archives of the late Dave Wittry) and to Fritz Prizivarra for the picture of Fig. 2. Cristina Villanova is thanked for providing the sample used to produce Fig. 7. John Bowles and Clive Walker are gratefully acknowledged for reviewing the manuscript.

REFERENCES

- ALBEE, A.L. & RAY, L. (1970). Correction factors for electron probe microanalysis of silicates, oxides, carbonates, phosphates and sulphates. *Anal Chem* **42**, 1408–1414.
- ARMIGLIATO, A., DESALVO, A., GARULLI, A. & ROSA, R. (1983). Thickness determination of Al films on Si by a Monte Carlo code using a secondary fluorescence correction. 10th ICXOM, Toulouse 5–9 September. *Journal de Physique* **43**(Suppl 2), C2-29–C2-32.
- ARMIGLIATO, A., DESALVO, A., RINALDI, R. & ROSA, R. (1979). Application of Monte Carlo technique to the electron probe microanalysis of ternary Si-B-O films on silicon. *J Phys D Appl Phys* **12**, 1299–1308.
- BARKSHIRE, I., KARDUCK, P., REHBACH, W.P. & RICHTER, S. (2000). High-spatial resolution low-energy electron beam X-ray microanalysis. *Mikrochim Acta* **132**, 113–128.
- BASTIN, G.F. & HEIJLIGERS, H.J.M. (2000a). A systematic database of thin-film measurements by EPMA—Part I—Aluminum films. *X-Ray Spectrom* **29**, 212–238.

- BASTIN, G.F. & HEIJLIGERS, H.J.M. (2000b). A systematic database of thin-film measurements by EPMA—Part II—Palladium films. *X-Ray Spectrom* **29**, 373–397.
- BASTIN, G.F., OBERNDORFF, P.J.T.L., DIJKSTRA, J.M. & HEIJLIGERS, H.J.M. (2001). Extension of PROZA96 to conditions of non-perpendicular incidence of the electron beam. *X-Ray Spectrom* **30**, 382–387.
- BASTIN, G.F., VAN LOO, F.J.J., VOSTERS, P.J.C. & VROLIJK, J.W.G.A. (1983). A correction procedure for characteristic fluorescence encountered in microprobe analysis near phase boundaries. *Scanning* **5**, 172–183.
- BERGER, D. & NISSEN, J. (2014). Measurement and Monte Carlo simulation of the spatial resolution in element analysis with the FEG-EPMA JEOL JXA-8530F. *IOP Conf Ser: Mater Sci Eng* **55**, 012002.
- BOWLES, J.F.W. (2015). Age dating from electron microprobe analyses of U, Th and Pb: Benefits and pitfalls. *Microsc Microanal*, this issue.
- BURDET, P., HÉBERT, C. & CANTONI, M. (2014). Enhanced quantification for 3D energy dispersive spectrometry: Going beyond the limitation of large volume of X-ray emission. *Microsc Microanal* **20**, 1544–1555.
- BUSE, B. & KEARNS, S. (2014). Importance of carbon contamination in high-resolution (FEG) EPMA of silicate minerals. *Microsc Microanal* **20**(Suppl 3), 704–705.
- CASTAING, R. (1951). *Application des sondes électroniques à une méthode d'analyse ponctuelle chimique et cristallographique*. Thèse présentée à la Faculté des Science de Université de Paris, le 8 Juin, Série A, No. 2423, No. d'ordre 3295.
- CHÖEL, M., DEBOUDT, K. & FLAMENT, P. (2007). Evaluation of quantitative procedures for X-ray microanalysis of environmental particles. *Microsc Res Tech* **70**, 996–1002.
- DONOVAN, J.J. (2011). High sensitivity EPMA: Past, present and future. *Microsc Microanal* **17**(Suppl 2), 560–561.
- DROUIN, D., COUTURE, A.R., JOLY, D., TASTET, X., AIMEZ, V. & GAUVIN, R. (2007). CASINO V2.42—A fast and easy-to-use modeling tool for scanning electron microscopy and microanalysis users. *Scanning* **29**, 92–101.
- DUNCUMB, P. (2001). Microprobe design in the 1950s: Some examples in Europe. *Microsc Microanal* **7**, 100–107.
- DUNCUMB, P. & STATHAM, P.J. (2002). Benefits of X-ray spectrum simulation at low energies. *Mikrochim Acta* **138**, 249–258.
- FIALIN, M., RÉMY, H., RICHARD, C. & WAGNER, C. (1999). Trace element analysis with the electron microprobe: New data and perspectives. *Am Mineral* **84**, 70–77.
- GANGULY, J., BHATTACHARYA, R.N. & CHAKRABORTY, S. (1988). Convolution effect in the determination of compositional profiles and diffusion coefficients in microprobe step scans. *Am Mineral* **73**, 901–909.
- GAUVIN, R., LIFSHIN, E., DEMERS, H., HORNY, P. & CAMPBELL, H. (2006). Win X-ray: A new Monte Carlo program that computes X-ray spectra obtained with a scanning electron microscope. *Microsc Microanal* **12**, 49–64.
- GOPON, P., FOURNELLE, J., SOBOL, P.E. & LLOVET, X. (2013). Low voltage electron-probe microanalysis of Fe-Si compounds using soft X-rays. *Microsc Microanal* **19**, 1698–1708.
- GRILLON, F. & PHILIBERT, J. (2002). The legacy of Raymond Castaing. *Mikrochim Acta* **138**, 99–104.
- HORNY, P., LIFSHIN, E., CAMPBELL, H. & GAUVIN, R. (2010). Development of a new quantitative X-ray microanalysis method for electron microscopy. *Microsc Microanal* **16**, 821–830.
- JERCINOVIC, M.J. & WILLIAMS, M.L. (2005). Analytical perils (and progress) in electron microprobe trace element analysis applied to geochronology: Background acquisition, interferences, and beam irradiation effects. *Am Mineral* **90**, 526–546.
- JERCINOVIC, M.J., WILLIAMS, M.L., ALLAZ, J. & DONOVAN, J.J. (2012). Trace analysis in EPMA. *IOP Conf Ser Mat Sci Eng* **32**, 012012.
- JERCINOVIC, M.J., WILLIAMS, M.L. & LANE, E.D. (2008). In-situ trace element analysis of monazite and other fine-grained accessory minerals by EPMA. *Chem Geol* **254**, 197–215.
- JONNARD, P., BRISSET, F., ROBAUT, F., WILLE, G. & RUSTE, J. (2014). An interlaboratory comparison of WDS-EDS quantitative X-ray microanalysis of a metallic glass. *X-Ray Spectrom* **44**, 24–29.
- KANE, W.T. (1974). A CAMAC automated electron microprobe. *9th Annual Conference of the Microbeam Analysis Society*, Tutorial and Proceedings, paper 32, July 22–26, Ottawa, Canada, pp. A–C.
- KEIL, K. (1973). Applications of the Electron Microprobe in Geology. In *Microprobe Analysis* (chapter 5 Andersen C.A. (Ed.), pp. 189–239). New York, USA: John Wiley & Sons.
- KIMURA, T., NISHIDA, K. & TANUMA, S. (2006). Spatial resolution of a wavelength-dispersive electron probe microanalyzer equipped with a thermal field emission gun. *Mikrochim Acta* **155**, 175–178.
- KUBO, Y., HAMARA, K. & URANO, A. (2013). Minimum detection limit and spatial resolution of thin-sample field-emission electron probe microanalysis. *Ultramicroscopy* **135**, 64–70.
- LAVRENT'EV, Y.G., KOROLYUK, V.N. & USOVA, L.V. (2004). Second generation of correction methods in electron probe X-ray microanalysis: Approximation models for emission depth distribution functions. *J Anal Chem* **59**, 600–616.
- LIMANDRI, S.P., BONETTO, R.D., GALVÁN-JOSA, V., CARRERAS, A.C. & TRINCAVELLI, J.C. (2012). Standardless quantification by parameter optimization in electron probe microanalysis. *Spectrochim Acta B* **77**, 44–51.
- LLOVET, X., FERNÁNDEZ-VAREA, J.M., SEMPAY, J. & SALVAT, F. (2005). Monte Carlo simulation of X-ray emission using the general-purpose code PENELOPE. *Surf Interface Anal* **37**, 1054–1058.
- LLOVET, X. & GALÁN, G. (2003). Correction of secondary X-ray fluorescence near grain boundaries in electron microprobe analysis: Application to thermobarometry of spinel lherzolites. *Am Mineral* **88**, 121–130.
- LLOVET, X., HEIKINHEIMO, E., NÚÑEZ, A., MERLET, C., ALMAGRO, J.F., RICHTER, S., FOURNELLE, J. & VAN HOEK, C.J.G. (2012). An interlaboratory comparison of EPMA analysis of alloy steel at low voltage. *IOP Conf Ser Mater Sci Eng* **32**, 012014.
- LLOVET, X. & MERLET, C. (2010). Electron probe microanalysis of thin films and multilayers using the computer program XFILM. *Microsc Microanal* **16**, 21–32.
- LLOVET, X., PINARD, P.T., DONOVAN, J.J. & SALVAT, F. (2012). Secondary fluorescence in electron probe microanalysis of material couples. *J Phys D Appl Phys* **45**, 225301.
- LLOVET, X., SALVAT, F., BOTE, D., SALVAT-PUJOL, F., JABLONSKI, A. & POWELL, C.J. (2014a). *NIST Database of Cross Sections for Inner-Shell Ionization by Electron and Positron Impact. Version 1.0*. Gaithersburg, Maryland: National Institute of Standards and Technology.
- LLOVET, X., SALVAT, F., POWELL, C.J. & JABLONSKI, A. (2014b). Cross sections for inner-shell ionization by electron impact. *J Phys Chem Ref Data* **43**, 013102.
- LLOVET, X., VALOVIRTA, E. & HEIKINHEIMO, E. (2000). Monte Carlo simulation of secondary fluorescence in small particles and at phase boundaries. *Mikrochim Acta* **132**, 205–212.
- LOVE, G., SEWELL, D.A. & SCOTT, V.D. (1983). An improved absorption correction for quantitative analysis. 10th ICXOM, Toulouse 5–9 September. *Journal de Physique* **43**(Suppl 2), C2-21–C2-24.

- MACRAE, C.M., WILSON, N.C. & TORPY, A. (2014). Multi-spectral electron microprobe—Now and the future. *Microsc Microanal* **20**(Suppl 3), 2164–2165.
- MANIGUET, L., ROBAUT, F., MEURIS, A., ROUSSEL-DHEBEY, F. & CHARLOT, F. (2012). X-ray microanalysis: The state of the art of SDD detectors and WDS systems on scanning electron microscopes (SEM). *IOP Conf Ser Mater Sci Eng* **32**, 012015–1–19.
- MARINENKO, R.B. & LEIGH, S. (2010). Uncertainties in electron probe microanalysis. *IOP Conf Ser Mater Sci Eng* **7**, 012017.
- MCSWIGGEN, P. (2014). Characterisation of sub-micrometer features with the FE-EPMA. *IOP Conf Ser Mater Sci Eng* **55**, 012009–1–12.
- MCSWIGGEN, P., ARMSTRONG, J.T. & NIELSEN, C. (2014). Strategies for low accelerating voltage X-ray microanalysis of sub-micrometer features with the FE-EPMA. *Microsc Microanal* **20**(Suppl 3), 688–689.
- MERLET, C. & BODINIER, J.-L. (1990). Electron microprobe determination of minor and trace transition elements in silicate minerals: A method and its application to mineral zoning in the peridotite nodule PHN 1611. *Chem Geol* **83**, 55–69.
- MERLET, C. & LLOVET, X. (2012). Uncertainty and capability of quantitative EPMA at low voltage—a review. *IOP Conf Ser Mater Sci Eng* **32**, 012016–1–15.
- MERLET, C., LLOVET, X. & SALVAT, F. (2004). Measurements of the surface ionization in multilayered specimens. *X-Ray Spectrom* **33**, 376–386.
- MORENO, I., ALMAGRO, J.F. & LLOVET, X. (2002). Determination of nitrogen in duplex stainless steels by EPMA. *Microchim Acta* **139**, 105–110.
- MORI, N., KUYPERS, S., TANAKA, T., NAKAJIMA, K. & KIMURA, T. (2011). Trace element analysis of sulphur in a Japanese sword. EMAS 2011 12th European Workshop on Modern Developments and Applications of Microbeam Analysis, Angers (France). 15–19 May 2011, Book of Abstracts. p. 369.
- MURATA, K., CVIKEVICH, S. & KUPTSIS, J.D. (1983). A Monte Carlo simulation approach to thin film electron microprobe analysis based on the use of Mott scattering cross section. 10th ICXOM, Toulouse 5–9 September. *Journal de Physique* **43**(Suppl 2), C2–13–C2–16.
- MYKLEBUST, R.L. & NEWBURY, D.E. (1995). Monte Carlo modeling of secondary fluorescence across phase boundaries in electron probe microanalysis. *Scanning* **17**, 235–242.
- NEWBURY, D.E. (2002). Barriers to quantitative electron probe X-ray microanalysis for low voltage scanning electron microscopy. *J Res Natl Inst Stand Technol* **107**, 605–619.
- NEWBURY, D.E. & RITCHIE, N.W.M. (2013). Is scanning electron microscopy/energy dispersive X-ray spectrometry (SEM/EDS) quantitative? *Scanning* **35**, 141–168.
- OHNUMA, I., ABE, S., SHIMENOCHI, S., OMORI, T., KAINUMA, R. & ISHIDA, K. (2012). Experimental and thermodynamic studies of the Fe–Si binary system. *ISIJ International* **52**, 540–548.
- PINARD, P.T. & RICHTER, S. (2014). Improving the quantification at high spatial resolution using a field emission electron microprobe. *IOP Conf Ser Mater Sci Eng* **55**, 012016–1–16.
- PISTORIUS, P.C. & VERMA, N. (2011). Matrix effects in the energy dispersive X-ray analysis of CaO–Al₂O₃–MgO inclusions in steel. *Microsc Microanal* **17**, 963–971.
- POUCHOU, J.L. (1996). Use of soft X-rays in microanalysis. *Mikrochim Acta* **13**(Suppl), 39–60.
- POUCHOU, J.L. (2002). X-ray microanalysis of thin surface films and coatings. *Microchim Acta* **138**, 133–152.
- POUCHOU, J.L. & PICOIR, F. (1983a). Extension des possibilités quantitatives de la microanalyse par une formulation nouvelle des effets de matrice. 10th ICXOM, Toulouse 5–9 September. *Journal de Physique* **43**(Suppl 2), C2–17–C2–20.
- POUCHOU, J.L. & PICOIR, F. (1983b). Analyse d'échantillons stratifiés à la microsonde électronique. 10th ICXOM, Toulouse 5–9 September. *Journal de Physique* **43**(Suppl 2), C2–47–C2–50.
- POUCHOU, J.L. & PICOIR, F. (1993). Electron probe X-ray microanalysis applied to thin surface films and stratified specimens. *Scan Microsc* **7**(Suppl), 167–189.
- POWNCBEY, M.I., MACRAE, C.M. & WILSON, N.C. (2007). Mineral characterisation by EPMA mapping. *Miner Eng* **20**, 444–451.
- PRÉT, D., SAMMARTINO, S., BEAUFORT, D., MEUNIER, A., FIALIN, M. & MICHOT, L.J. (2010). A new method for quantitative petrography based on image processing of chemical element maps: Part I. Mineral mapping applied to compacted bentonites. *Am Mineral* **95**, 1379–1388.
- REED, S.J.B. (2000). Quantitative trace analysis by wavelength-dispersive EPMA. *Microchim Acta* **132**, 145–151.
- REED, S.J.B. & LONG, J.V.P. (1963). Electron probe measurements near phase boundaries. In *Proc. ICXOM*, (Cosslett V.E. & Engström A. (Eds.), pp. 317–327). New York: Academic Press.
- RINALDI, R. (1978). Results and perspectives of the multiple and differentiated access to an electron microprobe laboratory. *J Microsc Spectrosc Electron* **3**, 12–13.
- RINALDI, R. (1979). La microanalisi elettronica: Strumentazione e applicazioni mineralogico-petrografiche. *Rend Soc It Mineral Petrol* **35**, 507–526.
- RINALDI, R. (1980). Automated WDS electron probe microanalysis: A floppy disk operative system. *Ultramicroscopy* **5**, 378.
- RINALDI, R. (1981). La microanalisi elettronica. In *Microscopia a Scansione e Microanalisi* (Capitolo 3, Parte II Microanalisi Armigliato A. & Valdrè e.U. (Eds.), pp. 242–294). Bologna, Italy: Centro Stampa Lo Scarabeo.
- RINALDI, R. (1985). Microanalisi-X: Recenti sviluppi e aspetti pratici. *Rend Soc It Mineral Petrol* **40**, 241–254.
- RINALDI, R. (1997). La microanalisi elettronica: Lineamenti storici e principi. *Plinius* (Ital Supp Eur J Mineral) **18**, 214–224.
- RITCHIE, N.W.M. (2005). A new Monte Carlo application for complex sample geometries. *Surf Interface Anal* **37**, 1006–1011.
- RITCHIE, N.W.M. & NEWBURY, D.E. (2012). Uncertainty estimates for electron probe X-ray microanalysis measurements. *Anal Chem* **84**, 9956–9962.
- RITCHIE, N.W.M., NEWBURY, D.E. & DAVIS, J.M. (2012). EDS measurements of X-ray intensity at WDS precision and accuracy using a silicon drift detector. *Microsc Microanal* **18**, 892–904.
- RO, C., OSAN, J., SZALÓKI, I., DE HOOG, J., WOROBIEC, A. & VAN GRIEKEN, R. (2003). A Monte Carlo program for quantitative electron-induced X-ray analysis of individual particles. *Anal Chem* **15**, 851–859.
- RUCKLIDGE, J.C., GASPARRINI, E., SMITH, J.V. & KNOWLES, C.R. (1971). X-ray emission microanalysis of rock-forming minerals. VIII. Amphiboles. *Can J Earth Sci* **8**, 1171–1183.
- SALVAT, F., FERNÁNDEZ-VAREA, J.M. & SEMPAY, J. (2011). *PENELOPE—A Code System for Monte Carlo Simulation of Electron and Photon Transport*. Issy-les-Moulineaux: OECD/Nuclear Energy Agency.
- SMITH, J.V. (1965). X-ray-emission microanalysis of rock forming minerals I. Experimental techniques. *J Geol* **73**, 830–864.
- SMITH, J.V. & RIBBIE, P.H. (1966). X-ray-emission microanalysis of rock forming minerals III. Alkali feldspars. *J Geol* **74**, 197–216.
- SOBOLEV, A.V., HOFMANN, A.W., KUZMIN, D.V., YAXLEY, G.M., ARNDT, N.T., CHUNG, S.-L., DANYUSHEVSKY, L.V., ELLIOTT, T., FREY, F.A., GARCIA, M.O., GURENKO, A.A., KAMENETSKY, V.S., KERR, A.C., KRIVOLUTSKAYA, N.A., MATVIENKOV, V.V., NIKOGOSIAN, I.K., ROCHOLL, A., SIGURDSSON, I.A., SUSHCHEVSKAYA, N.M. & TEKLY, M.

- (2007). The amount of recycled crust in sources of mantle-derived melts. *Science* **316**, 412–417.
- SORBIER, L., ROSENBERG, E. & MERLET, C. (2004). Microanalysis of porous materials. *Microsc Microanal* **10**, 745–752.
- STATHAM, P., DUNCUMB, P. & LLOVET, X. (2014). Systematic discrepancies in Monte Carlo predictions of K-ratios emitted from thin films on substrates. *IOP Conf Ser Mater Sci Eng* **32**, 012024.
- STATHAM, P. & HOLLAND, J. (2014). Prospects for higher spatial resolution quantitative X-ray analysis using transition element L-lines. *IOP Conf Ser Mater Sci Eng* **55**, 012017.
- STUMPFL, E.F. (1961). Some new platinum-rich minerals identified with the electron microanalyser. *Mineralog Mag* **32**, 833–847.
- STUMPFL, E.F. & CLARK, A.M. (1965). *Electron-Probe Microanalysis of Gold-Platinoid Concentrates from Southeast Borneo*, vol. 74, pp. 933–946. Inst Mining & Metallurg Trans.
- TAKAHASHI, H., MCSWIGGEN, P. & NIELSEN, C. (2014a). A unique wavelength-dispersive soft X-ray emission spectrometer for electron probe X-ray microanalyzers. *Microsc Anal* **15**, S5–S8.
- TAKAHASHI, H., MURANO, T., TAKAKURA, M., HANDA, N., TERAUCHI, M., KOIKE, M., KAWACHI, T., IMAZONO, T., HASEGAWA, N., KOEDA, M., NAGANO, T., SASAI, H., OUE, Y., YONEZAWA, Z. & KURAMOTO, S. (2014b). Characteristic features and applications of a newly developed wavelength dispersive soft X-ray emission spectrometer for electron probe X-ray microanalyzers and scanning electron microscopes. *JEOL News* **49**, 73–80.
- TERAUCHI, M., KOSHIYA, S., SATOH, F., TAKAHASHI, H., HANDA, N., MURANO, T., KOIKE, M., IMAZONO, T., KOEDA, M., NAGANO, T., SASAI, H., OUE, Y., YONEZAWA, Z. & KURAMOTO, S. (2014). Chemical state information of bulk specimens obtained by SEM-based soft-X-ray emission spectrometry. *Microsc Microanal* **20**, 692–697.
- TRINCAVELLI, J.C., LIMANDRI, S.P. & BONETTO, R.D. (2014). Standardless quantification methods in electron probe microanalysis. *Spectrochim Acta B* **101**, 76–85.
- WADE, J. & WOOD, B. (2012). Metal–silicate partitioning experiments in the diamond anvil cell: A comment on potential analytical errors. *Phys Earth Plan Inter* **192–193**, 54–58.
- WILLICH, P. & BETHKE, R. (1996). Practical aspects and applications of EPMA at low electron energies. *Mikrochim Acta* **13**(Suppl), 631–638.
- WUHRER, R., MORAN, K. & MORAN, L. (2006). Characterisation of materials through X-ray mapping. *Mater Forum* **30**, 63–70.
- ZIEBOLD, T.H.O. (1967). Precision and sensitivity in electron microprobe analysis. *Anal Chem* **39**, 858–861.